

Supporting information

Synergistic Effect of WO₃ on Physico-chemical, Physico-mechanical, Hydrophobic, and Anticorrosive Performance of Poly-(*melamine-co-formaldehyde*)-Cured *Pithecellobium dulce*-Alkyd Nanocomposite Coatings

Abu Darda^{1*}, Nitya Nand Gosvami¹, Weqar Ahmad Siddiqi²

¹*Department of Materials Science and Engineering, Indian Institute of Technology, Delhi*

²*Department of Applied Sciences and Humanities, Jamia Millia Islamia, New Delhi-110025, India*

Number of pages: 5 (S-1 to S-6)

Number of Figures: 2 (S-1 and S-2)

Number of tables: 4 (S-1 to S-4)

Number of Section: 1 (S-1)

Section S-1. FTIR Spectroscopic Analysis of WO₃ Nanoparticles

The FT-IR spectrum of WO₃ nanoparticles, as shown in Figure S-1, displays characteristic peaks at 940.90 cm⁻¹ and 678.84 cm⁻¹ corresponding to the asymmetric and symmetric stretching vibrations of crystalline W=O and O-W-O bonds, respectively. Additionally, the peak observed at 1626.74 cm⁻¹ is attributed to the presence of hydroxyl groups bonded to tungsten atoms, while the peak at 3444.01 cm⁻¹ is likely due to surface moisture associated with these hydroxyl groups. These observations confirm the successful formation of WO₃ nanoparticles (Figure S-1) [1–4].

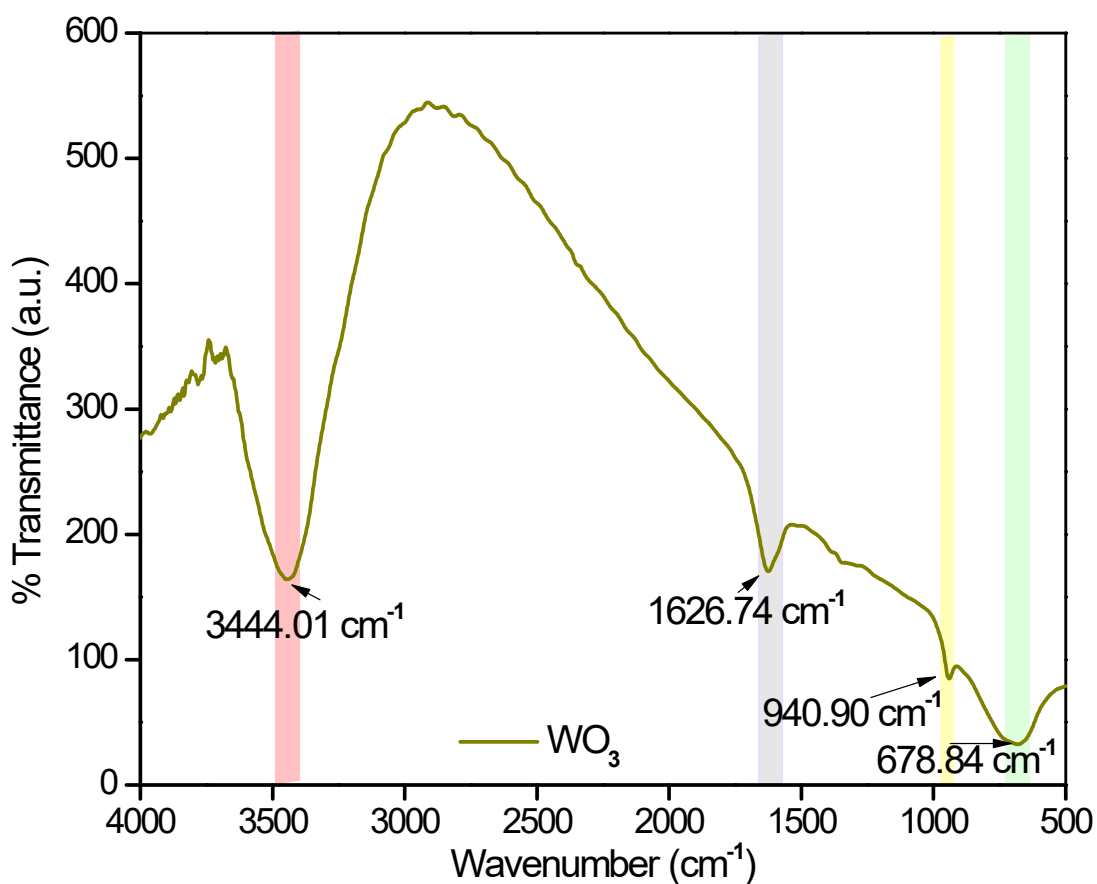


Figure S-1 FTIR spectra confirming the functional characteristics of WO₃ nanoparticles.

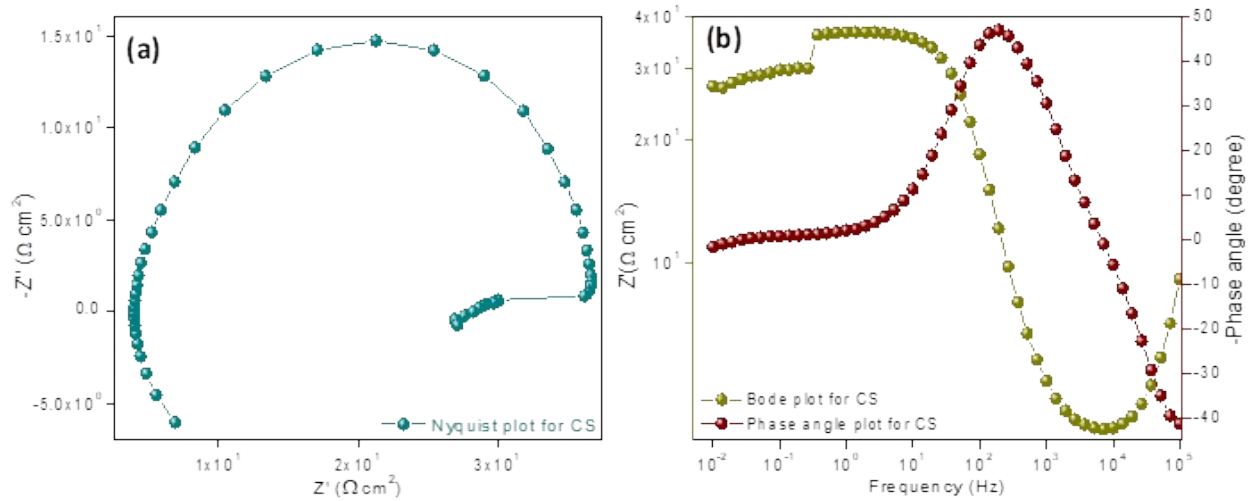


Figure S-2 (a) Nyquist and (b) [Bode and phase angle] plots of uncoated carbon steel (CS) in 5 wt.% NaCl solution.

Table S-1 Physico-chemical parameters of PDA, PDA-PMF₈₀, and WO₃@PDA-PMF₈₀ nanocomposite coatings.

Resin Code	PDA	PDA-PMF ₈₀	WO ₃ @PDA-PMF ₈₀
Acid value (mg KOH/g)	0.025	0.019	0.011
Refractive Index (25°C)	1.471	1.495	1.513
Specific gravity (g/ml at 25C)	1.09	1.13	1.25

Table S-2 Physico-mechanical parameters of PDA, PDA-PMF₈₀, and WO₃@PDA-PMF₈₀ nanocomposite coatings.

Properties/Coating's Codes	PDA	PDA-PMF ₈₀	WO ₃ @PDA-PMF ₈₀
Bend test (1/8'' inch)	passed	passed	Passed
Coating thickness (μm)	85	89	91
Cross hatch test	Passed	Passed	Passed
DTH time (h)	48	30	24
DTT time (min)	54	36	30
Gloss (45°)	68	81	83

Impact test (250, lb.inch⁻¹)	passed	passed	Passed
Scratch hardness (Kg)	5.5	10.5	12.0

Table S-3. Comparative thermogravimetric parameters of PDA-PMF₈₀ and WO₃@PDA-PMF₈₀ nanocomposite coatings derived from TGA analysis

Thermal Parameters	PDA-PMF₈₀ (°C)	WO₃@PDA-PMF₈₀ (°C)
Initial decomposition temperature (IDT, °C)	~136	~138
Onset degradation temperature, T _{onset} (°C)	~304	~336
Temperature at 5 wt.% loss, T _{d5} / T ₅ (°C)	~304	~336
First major degradation temperature (°C)	~304	~336
Second major degradation temperature (°C)	~428	~465
Maximum weight loss (%)	~85	~78
Residual char at 800 °C (%)	~5	~12
Thermal stability behavior	Moderate	Enhanced
Barrier/char-forming behavior	Lower	Higher
Overall thermal resistance	Lower	Improved due to WO ₃ incorporation

Where;

IDT = Initial decomposition temperature;

T_{onset} = onset degradation temperature;

T_{d5} = temperature corresponding to 5 wt.% weight loss.

The higher residual char yield and delayed degradation temperatures observed for WO₃@PDA-PMF₈₀ indicate improved thermal stability due to the incorporation of thermally stable WO₃ nanofillers within the polymer matrix.

Table S-4 Comparison of anticorrosive performance of WO₃@PDA-PMF₈₀ nanocomposite coatings with reported systems in the literature.

Sr No	Coating system	Immersion medium	Icorr (Acm ⁻²)	Corrosion rate (mpy)	Ref.
1	WO ₃ @PDA-PMF ₈₀	5wt% NaCl	1.56×10 ⁻⁷	4.81×10 ⁻⁴	P.S.
2	WCA-BMF ₈₀	5wt% NaCl	4.50 ×10 ⁻⁷	5.23×10 ⁻³	[5]
3	Alk-DDS—Ppy-PSCeO ₂	1.5 M NaCl	3.0×10 ⁻¹	9.85×10 ⁻¹	[6]
4	ASAR/10%SiO ₂	3.5wt% NaCl	7.03×10 ⁻⁷	1.09×10 ⁻³	[7]
5	NLA-IPTES-III	3.5wt% NaOH	7.20×10 ⁻⁷	8.00×10 ⁻⁴	[8]

References

- [1] J.R. Xavier, Effect of surface modified WO₃ nanoparticle on the epoxy coatings for the adhesive and anticorrosion properties of mild steel, *Journal of Applied Polymer Science* 137 (2020) 1–10. <https://doi.org/10.1002/app.48323>.
- [2] K. Pandurangarao, V. Ravi Kumar, Preparation and characterization of nanocrystalline tungsten oxide thin films for electrochromic devices: Effect of deposition parameters, *Materials Today: Proceedings* 19 (2019) 2596–2603. <https://doi.org/10.1016/j.matpr.2019.10.093>.
- [3] S.R. Arunima, M.J. Deepa, C. V. Geethanjali, V.S. Saji, S.M.A. Shibli, Tuning of hydrophobicity of WO₃-based hot-dip zinc coating with improved self-cleaning and anti-corrosion properties, *Applied Surface Science* 527 (2020) 146762. <https://doi.org/10.1016/j.apsusc.2020.146762>.
- [4] A. Darda, H. Khatoon, W.A. Siddiqi, S. Ahmad, Polythiophene enveloped tungsten-oxide hybrid nanofillers dispersed oleo (Pithecellobium Dulce seed oil) polyurethane bi-functional nanocomposite coatings, *Progress in Organic Coatings* 172 (2022) 107038. <https://doi.org/10.1016/J.PORGCOAT.2022.107038>.
- [5] S. Pathan, S. Ahmad, Synthesis, characterization and the effect of the s-triazine ring on physico-mechanical and electrochemical corrosion resistance performance of waterborne castor oil alkyd, *Journal of Materials Chemistry A* 1 (2013) 14227–14238.

<https://doi.org/10.1039/c3ta13126b>.

- [6] M.I. Bakshi, S. Ahmad, In situ synthesis of high-performance 4,4'-diaminodiphenylsulfone modified oleo-alkyd nanocomposite coatings: Role of hybrid nanofillers on physico-mechanical, hydrophobic and corrosion protective performance, *New Journal of Chemistry* 44 (2020) 17924–17937. <https://doi.org/10.1039/d0nj03407j>.
- [7] S. Zhong, J. Li, Y. Cai, L. Yi, Novel surfactant-free waterborne acrylic-silicone modified alkyd hybrid resin coatings containing nano-silica for the corrosion protection of carbon steel, *Polymer-Plastics Technology and Materials* 58 (2019) 866–878. <https://doi.org/10.1080/03602559.2018.1542711>.
- [8] S. Pathan, S. Ahmad, Synergistic Effects of Linseed Oil Based Waterborne Alkyd and 3-Isocyanatopropyl Triethoxysilane: Highly Transparent, Mechanically Robust, Thermally Stable, Hydrophobic, Anticorrosive Coatings, *ACS Sustainable Chemistry and Engineering* 4 (2016) 3062–3075. <https://doi.org/10.1021/acssuschemeng.6b00024>.